Step ordering induced by nonplanar patterning surfaces

2008 J. Phys.: Condens. Matter 20 095003

(http://iopscience.iop.org/0953-8984/20/9/095003)

J. Phys.: Condens. Matter **20** (2008) 095003 (6pp) doi:10.1088/0953-8984/20/9/095003

Step ordering induced by nonplanar patterning surfaces

X Tan, M Q Cai and G W Yang[1]

State Key Laboratory of Optoelectronic Materials and Technologies, Institute of Optoelectronic and Functional Composite Materials, School of Physics Science and Engineering, Zhongshan University, Guangzhou 510275, People's Republic of China

E-mail: stsygw@mail.sysu.edu.cn

Received 2 November 2007, in final form 14 December 2007
Published 4 February 2008
Online at stacks.iop.org/JPhysCM/20/095003

Abstract

Kinetic Monte Carlo simulations are carried out to address the influence of edge diffusion, terrace length, and lateral mass flux on the profiles of step ordering on nonplanar patterning surfaces. It is found that that the appearance of edge diffusion significantly affects both the recess width and the recess length, and a profile transition from the concave undulation to the straight train can be induced by increasing the edge diffusion rate. The length of the recess can be severely tuned by changing either the terrace length or the lateral mass flux.

(Some figures in this article are in colour only in the electronic version)

1. Introduction

Low-dimensional semiconductor structures such as quantum wires (QWs) and dots (QDs) have received considerable attention recently due to their interesting physical properties and potential applications in high performance devices [1–3]. Fabrications of uniform arrays of QWs and QDs have been achieved with metal–organic vapor-phase epitaxy (MOVPE) and molecular-beam epitaxy (MBE) on substrates patterned with V grooves [4, 5] and pyramidal recesses [6, 7]. Recently, an especially striking phenomenon of step ordering during MOVPE on nonplanar patterning of GaAs surfaces was reported [8]. Volta *et al* [9] studied the underlying mechanisms and found that the width of the ridges between neighboring V grooves and the kinetics of interface mass migration between the ridge and the bounding sidewalls of the V groove determine the unusual step ordering on ridges of GaAs(001) V-grooved vicinal substrates during MOVPE. Additionally, the significant effects of edge diffusion and terrace length on planar surfaces and unpatterned vicinal (or stepped) surfaces have been extensively studied in previous works [10–14]. However, there is no study involving the diffusion rate of atoms along the step edges, the length of terraces separated by monatomic steps, and the flux rate of lateral mass flux from the V groove factors that may influence the profiles of step ordering on nonplanar patterning surfaces to date.

In this contribution, we perform the kinetic Monte Carlo (KMC) simulations to study the influence of three important factors, i.e. the edge diffusion, the terrace length, and the flux rate of lateral mass flux from the V grooves, on the profiles of step ordering on nonplanar patterning surfaces. Importantly, our studies suggest the possibility of designing patterns that channel mass into predetermined regions of the substrate, which is useful for preparation of improved nanostructures such as QWs, QDs, quantum wells, and fractional monolayer superlattices.

2. KMC simulations

Here we apply a modified solid-on-solid model with various deposition and diffusion processes based on our previous work [15–17]. The KMC simulations are carried out on simple cubic vicinal surfaces between neighboring V grooves as shown in figure 1. Since the dissociation rate of trimethylgallium on the sidewalls of the {111}V groove is the higher than that on the (001) ridge upon the deposition process on the nonplanar patterning surface [9, 18], we consider a lateral mass flux from the V grooves which is not considered in the unpatterned models. Thus, in our simulations, atoms are deposited randomly on the surface and at the V-groove boundary sites at different average fluxes F_0 and F_e, respectively. Noted that F_e denotes the lateral mass flux from the V grooves due to the higher dissociation rate of trimethylgallium on the sidewalls of groove.

[1] Author to whom any correspondence should be addressed.

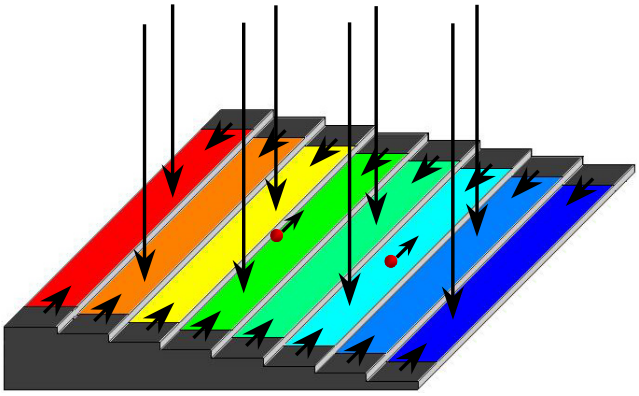

Figure 1. A schematic representation showing the simulation model of step ordering on the nonplanar patterning surface. (1) Deposition, (2) lateral mass flux from the V grooves, (3) diffusion of free adatom, and (4) edge diffusion of adatom. Different colors/levels of gray represent different terraces on the nonplanar patterning surface, and the (lightest) gray represents the V grooves in the lateral direction. The red/black circles denote the adatoms.

Volta *et al* [9] considered that the diffusion barrier of an adatoms is $E_S + nE_N$ upon the diffusion process, where E_S and E_N denote the energy barrier for free adatom diffusion and the energy of the bonds formed by an adatom with its n nearest neighbors ($n = 1$–4), respectively. Therefore, the diffusion rate of adatoms along the step edges is determined by E_S and E_N, and the influence of the edge diffusion cannot be studied in their model.

In order to investigate the influence of the diffusion rate of adatoms along the step edges on the profiles of step ordering on the nonplanar patterning surfaces, we improve Volta's model to simulate the diffusion process. The free adatoms can hop to the nearest neighbor sites with a diffusion rate D. Once a free adatom reaches a step edge, it can diffuse along the step edge and not be allowed to detach again [10, 11]. In our model, both the diffusion of a step-edge atom that has only one nearest neighbor and the step-edge atom's diffusion past the outside corner are allowed with the edge diffusion rate D_e. Once the step-edge atom reaches a site, it has more than one nearest neighbor, i.e. it reaches a kink (or inside corner) along the step edge, and becomes immobile [10, 11].

Additionally, we consider the diffusion of a step-edge atom that has more than one nearest neighbor in our simulations, and find that the influences of the diffusion on the simulation results are very small. The steps approach the edges of the ridge at right angles on the nonplanar patterning surface, which can result in the adatoms migrating along the step edges and can be reflected at the V-groove boundary back toward the interior of the ridge [9]. This result suggests that the V-groove boundary is a reflecting boundary, which is not considered in the unpatterned models. Namely, the diffusion of adatoms across the V-groove boundary, from the inside to the outside of the ridge, is prohibited, and the adatoms at the V-groove boundary sites can only diffuse along the V-groove boundary or toward the interior of the ridge.

The simulation time, Δt (the unit time is the second), taken for any given event to occur, is simply the reciprocal of the sum of the rates of all the events in the system. For mathematical completeness, a factor of $-\ln(R)$ is included, in which R is a random number between zero and unity. The full expression of the time increment is given as

$$\Delta t = \left[\sum_{i=1}^{n} v_i\right]^{-1} (-\ln R) \qquad (1)$$

where v_i is the rate for event i to occur.

The KMC simulations are carried out on a square 80×80 lattice array of equidistant straight step trains on the terrace (figure 2(a)) with the terrace length ranging from $2a$ to $16a$ in order to investigate the terrace length effects on the step ordering. Namely, the ridge width between neighboring V grooves is $80a$ in our simulations. Periodic boundary conditions are applied along the step train and the reflecting boundary conditions are imposed in the lateral direction. All the results shown here are obtained with $F_0 = 1$ ML s^{-1},

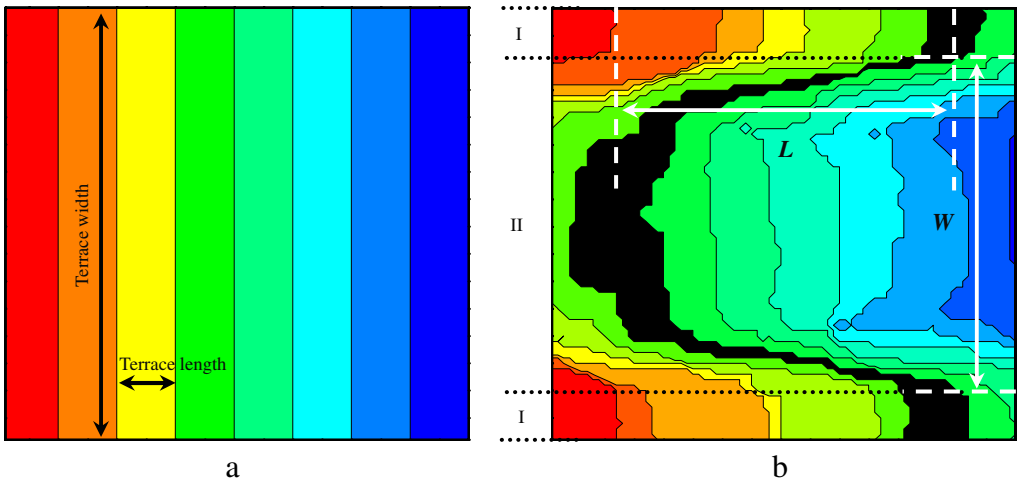

Figure 2. Typical (a) initial and (b) final step profiles of step ordering induced by nonplanar patterning surfaces with eight equidistant straight steps with the terrace length $10a$ obtained at $D = 1\times 10^6$ s^{-1}, $D_e = 1\times 10^4$ s^{-1}, $F_0 = 1$ ML s^{-1}, $F_e = 0.1$ ML s^{-1}, and $\theta = 10$ ML. The black shows the profile of a step after deposition of 10 ML, and the recess length (L) and recess width (W) are defined.

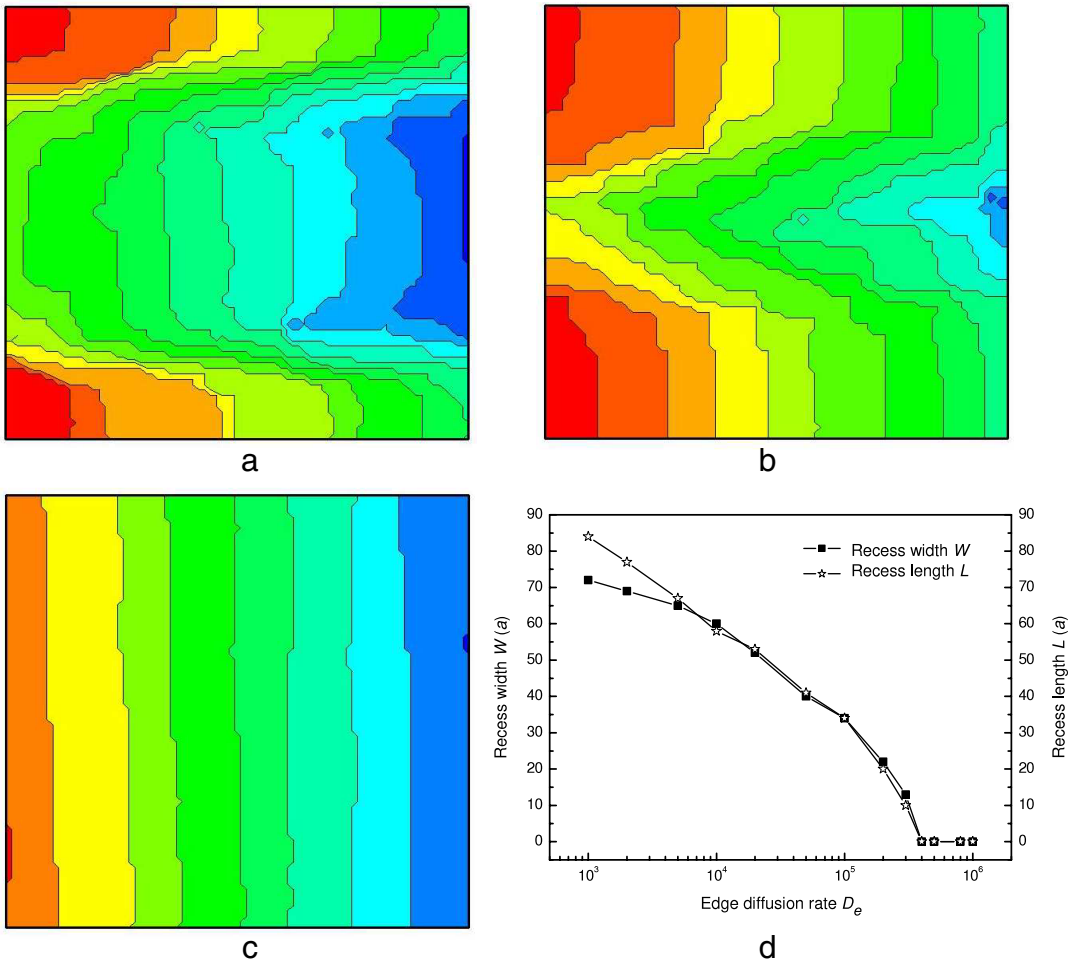

Figure 3. (a)–(c) The step profiles on nonplanar patterning surfaces with eight equidistant straight steps obtained at $D = 1 \times 10^7 s^{-1}$, $F_0 = 1$ ML s^{-1}, $F_e = 0.1$ ML s^{-1}, and $\theta = 10$ ML, but at three different edge diffusion rates: (a) $D_e = 1 \times 10^4$ s^{-1}, (b) $D_e = 1 \times 10^5$ s^{-1}, and (c) $D_e = 1 \times 10^6$ s^{-1}. (d) The width and length of the recess in the center of the ridge as a function of edge diffusion rate.

$D = 10^6$–10^8 s^{-1}, and the coverage $\theta = 10$ ML. In order to investigate the effects of step edge diffusion and lateral mass flux from the V grooves, we choose D_e ranging from 10^3 to 10^6 s^{-1}, and F_e ranging from 0.02 to 0.2 ML s^{-1}, respectively. All the data reported in our case are averaged from the results of 50 simulation runs in order to improve the observed statistics.

3. Results and discussions

Figure 2 shows a typical step ordering induced by nonplanar patterning surfaces. It can be seen that in this case the nucleation on the terrace is virtually absent and the thin film grows in the step flow mechanism. The step profile of the ridge translates from the equidistant straight steps (figure 2(a)) into the pronounced concave undulation with the recessed profile in the center of the ridge after the deposition of 10 ML (figure 2(b)). These results are consistent with the experiment and simulation results [9]. To simplify our discussions, we divide the ridge into two regions: the edge region I, where the steps are perpendicular to the boundary of V grooves, and the recess region II, with the recessed profile in the center of the ridge, as shown in figure 2(b). In addition, we define the recess length (L) as the distance between the two midlines (along the step train) of a terrace in regions I and II, and the recess width (W) is the distance between the two boundaries of regions I and II of a terrace, which are clearly shown in figure 2(b). The step ordering induced by the nonplanar patterning surfaces can be understood by considering the effects of the lateral mass flux from the V grooves and the reflecting boundaries at the V grooves [9]. These effects induce that the thin film growth rate in the edge region is much faster than that in the recess region, which results in a concave undulation along the step train. Moreover, we simulate the step ordering at diffusion rate D ranging from 10^6 to 10^8 s^{-1}, and find that the influence of the diffusion rate on step profile can be ignored.

Volta *et al* [9] investigated the underlying mechanisms of the step ordering during MOVPE on the nonplanar patterning surfaces, and found a profile transition from the straight train to the concave undulation with increasing the ridge widths. However, other factors, which might influence the step profiles on the nonplanar patterning surfaces and induce the profile transition between the straight train and the concave undulation, were not investigated in their work. Accordingly,

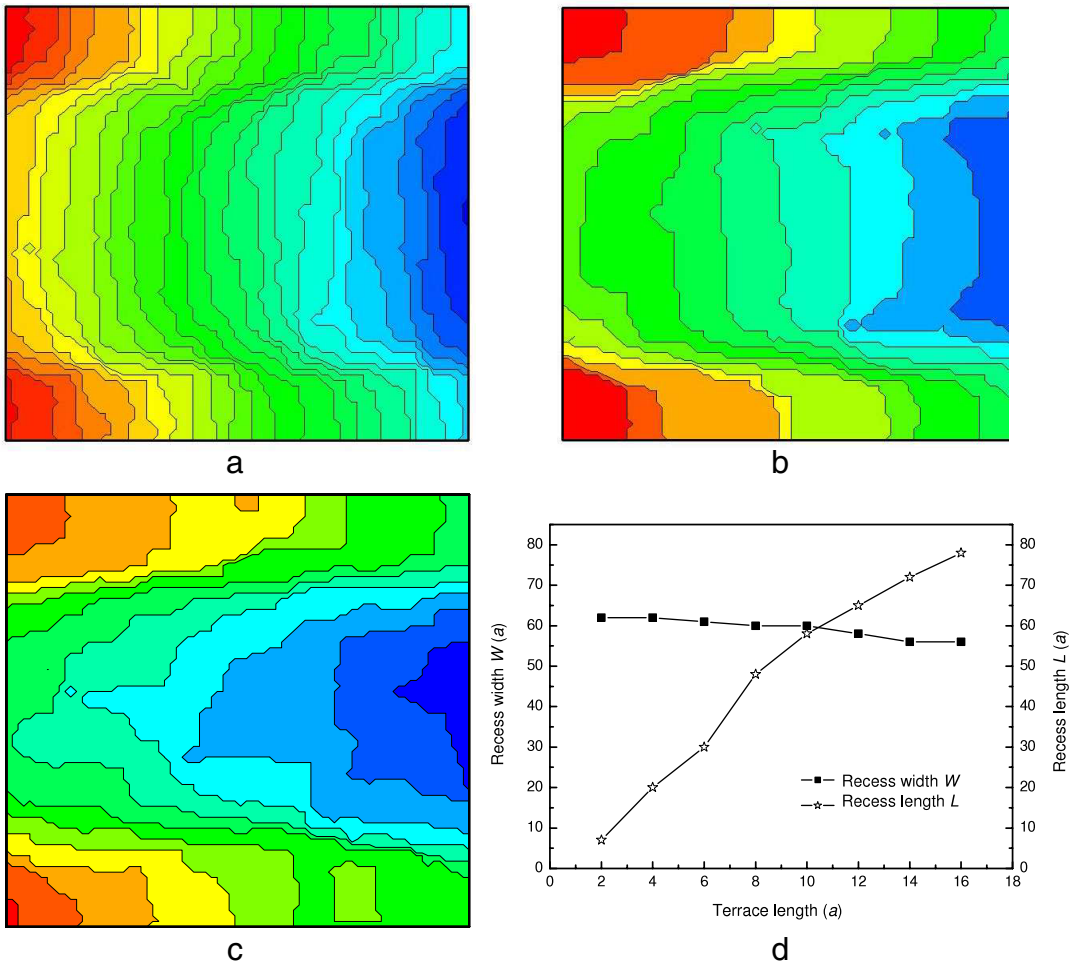

Figure 4. (a)–(c) The step profiles obtained at different terrace lengths: (a) $4a$, (b) $10a$, (c) $16a$. Here we use $D = 1 \times 10^6 \mathrm{s}^{-1}$, $D_e = 1 \times 10^4\ \mathrm{s}^{-1}$, $F_0 = 1$ ML s^{-1}, $F_e = 0.1$ ML s^{-1}, and $\theta = 10$ ML. (d) The width and length of the recess as a function of terrace length.

we carry out KMC simulations to study the influences of the edge diffusion, the terrace length, and the flux rate of lateral mass flux from the V grooves on the profiles of the step ordering on the nonplanar patterning surfaces based on the proposed model, which have not been involved in Volta's studies [9] and other previous works.

Figures 3(a)–(c) show the edge diffusion rate dependence of the step profile on the nonplanar patterning surfaces. At the low edge diffusion rate $D_e = 1 \times 10^4\ \mathrm{s}^{-1}$, the step profile is typically a concave undulation with recessed profile in the center of the ridge and the width of the recess is large (figure 3(a)). At the high edge diffusion rate $D_e = 1 \times 10^6\ \mathrm{s}^{-1}$, the steps are essentially straight and no recess can be seen along the step train (figure 3(c)). The transition from the concave undulation to the straight train takes place approximately at $D_e = 4 \times 10^5\ \mathrm{s}^{-1}$. Figure 3(b) shows that for the step profile at $D_e = 1 \times 10^5\ \mathrm{s}^{-1}$ (just below the transition edge diffusion rate) the step profile is still the concave undulation, though the width of the recess in the center of the ridge decreases. This can be seen more quantitatively in figure 3(d), where we show the width and length of the recess in the center of the ridge as a function of edge diffusion rate. We clearly see that both the width and length of the recess decrease dramatically with the edge diffusion rate increasing, and then approach zero after the transition edge diffusion rate. These results indicate that the step edge diffusion has a significant influence on both the width and the length of the recess, and can be used as an additional parameter to control the step ordering on nonplanar patterning surfaces in experiment.

Moreover, we can use figure 3(d) to predict the transition point for different ridge widths when the ridge widths are smaller than $80a$. For example, when the edge diffusion rate is $1 \times 10^4\ \mathrm{s}^{-1}$, the recess width is about $60a$ (in figure 3(d)), and the width of the edge regions on each side is about $10a$. Thus, we can predict that the transition point for the ridge width of $20a$ is approximately $1 \times 10^4\ \mathrm{s}^{-1}$.

The physical mechanisms of these interesting findings are attributed to diffusion of adatoms from the edge region to the recess region. For the small edge diffusion rate, adatoms from the lateral mass flux of the V grooves can attach to the step edges near the V-groove boundary, but the diffusion of the step-edge atoms along the step edges is restrained. This results in the edge region being small and the recess region large. For the large edge diffusion rate, the step-edge atoms adatoms can diffuse from the high growth rate region (i.e. the edge region) to the low growth rate region (i.e. the recess region), which leads

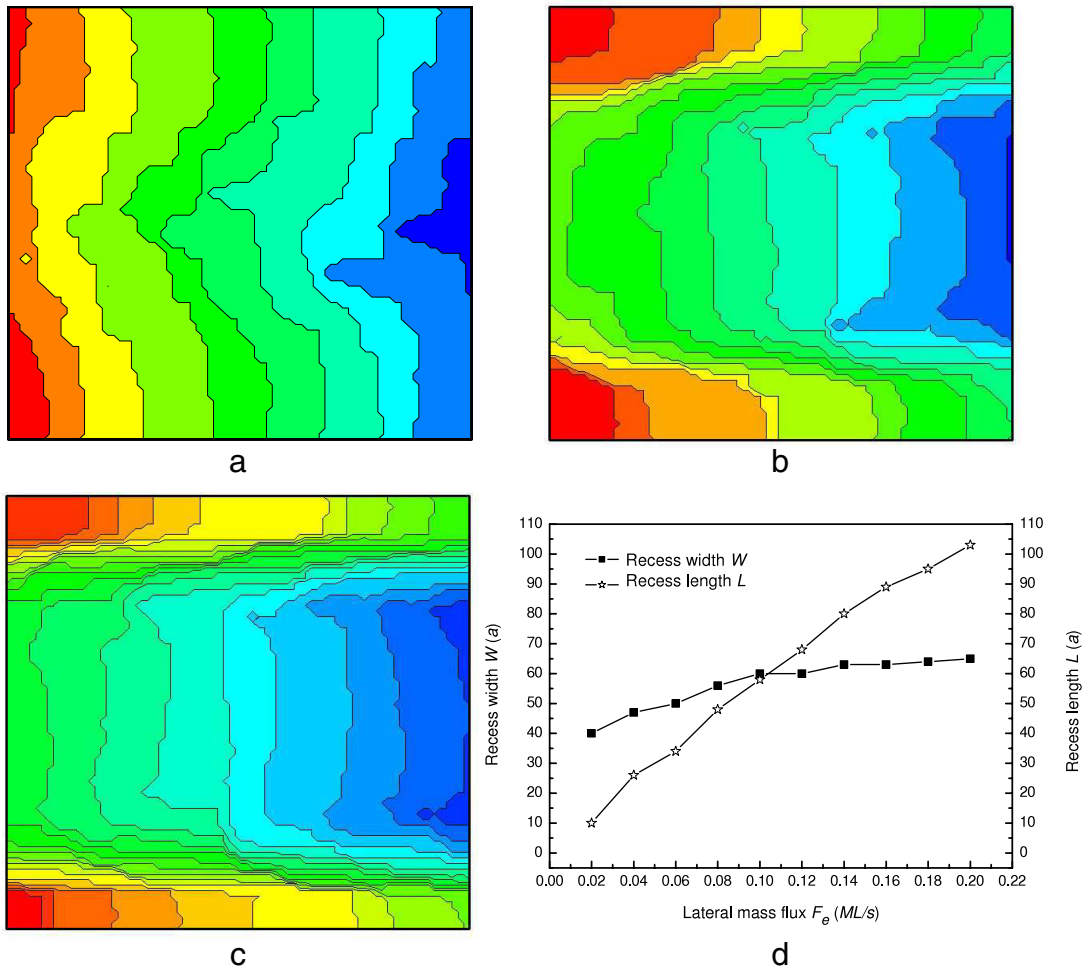

Figure 5. (a)–(c) The lateral mass flux dependence of the step profile on nonplanar patterning surfaces with eight equidistant straight steps obtained at $D = 1 \times 10^6$ s^{-1}, $D_e = 1 \times 10^4$ s^{-1}, $F_0 = 1$ ML s^{-1}, and $\theta = 10$ ML, but with three different lateral mass fluxes: (a) 0.02 ML s^{-1}, (b) 0.1 ML s^{-1}, and (c) 0.2 ML s^{-1}. (d) The width and length of the recess as a function of lateral mass flux.

to the edge region increasing and the recess region decreasing. Thus, the width of the recess decreases. On the other hand, due to the edge region adatom diffusion to the recess region, the difference of the thin film growth rates between the edge region and the recess region decreases. This result causes the decrease of the recess length. In particular, when the edge diffusion rate is sufficiently large, adatoms can rapidly diffuse from the edge region to the recess region, which leads to an equal growth rate between the edge region and the recess region. Therefore, the step profile translates from the concave undulation into essentially equidistant straight steps.

In fact, some methods can change the edge diffusion rate in experiments. For example, we can introduce a surfactant, as it has essentially no effect on the diffusion on the surface, and binds predominantly at the steps to suppress (or enhance) the edge diffusion [10, 19]. Additionally, in the growth of compound semiconductors such as III/V semiconductors, a change of the ratio of the groups III–V can be used to change the surface reconstructions, which leads to different microscopic structures along the step corresponding to different edge diffusion rates [10, 20]. Thus, the change of the edge diffusion can be achieved by changing the III/V ratio.

Figures 4(a)–(c) display the step profiles obtained at the different terrace lengths, ranging from $2a$ to $16a$. For small terrace length $4a$ (figure 4(a)), there is a pronounced concave undulation with a wide recess, but the length of the recess is small. When increasing the terrace length to $10a$ (figure 4(b)), the change of the recess width is small, while the recess length increase dramatically, indicating that the influence of terrace length on the recess length is significant. Further increasing the terrace length to $16a$ (figure 4(c)), some islands nucleate on the terraces, and the thin film growth translates from the step flow mechanism to the two-dimensional island nucleation and growth mechanism [13, 14, 21]. The width and length of the recess as a function of terrace length are shown in figure 4(d). It can be seen from the figure that the recess length increases dramatically from $7a$ to $78a$ with the terrace length increasing, while the recess width is approximately constant for various terrace lengths. The terrace length dependence described above can be understood by considering the effects of the lateral mass flux.

For a small terrace length, the number of lateral edge sites for each step edge is relatively small (about four lateral edge sites for a terrace length of $4a$), so that the number of adatoms

from lateral mass flux for each step edge is correspondingly small. For a large terrace length, the number of lateral edge sites for each step edge is large (about 10 lateral edge sites for terrace length of $10a$), and the number of adatoms from lateral mass flux for each step edge is large. Thus, the thin film growth rate of the edge region for large terrace length is much faster than that for small terrace length, which leads to the increase of recess length as the terrace length increases. On the other hand, as the edge diffusion rate is constant for various terrace lengths, the edge region is fixed and the widths of the recess are equal for various terrace lengths.

Figures 5(a)–(c) show the lateral mass flux dependence of the step profile on nonplanar patterning surfaces with eight equidistant straight steps. For small lateral mass flux $F_e = 0.02$ ML s^{-1}, the step profile is a concave undulation and the length of the recess is small (figure 5(a)). As the lateral mass flux increases, $F_e = 0.1$ ML s^{-1}, the recess length increases significantly, while the recess width is maintained (figure 5(b)). For large lateral mass flux $F_e = 0.2$ ML s^{-1}, the length of the recess becomes very large while the change of recess width is still small compared with small lateral mass flux (figure 5(c)), indicating that the effect of lateral mass flux on the recess length is very large. This can be seen more quantitatively in figure 5(d), where we show the width and length of the recess as a function of lateral mass flux. We can clearly see that the length of the recess increase rapidly with the lateral mass flux increasing, while the recess width is approximately constant for various lateral mass fluxes. This is plausible since the effects of lateral mass flux on the thin film growth rate of the edge region increase with the lateral mass flux increasing, resulting in the dramatic increase of the recess length. On the other hand, as the edge diffusion rate is fixed, the change of recess width can be ignored.

4. Conclusion

In summary, the KMC simulations of the influence of edge diffusion, terrace length, and flux rate of lateral mass flux on the profiles of step ordering on nonplanar patterning surfaces have demonstrated that the edge diffusion appears to significantly influence both the recess width and the recess length, and a profile transition from concave undulation to straight train can be induced by increasing the edge diffusion rate. The length of the recess can be strongly tuned by changing either the terrace length or the lateral mass flux.

Acknowledgments

The National Science Foundation of China (50525206 and U0734004) and the Ministry of Education (106126) supported this work.

References

[1] Weisbuch C and Vinter B 1991 *Quantum Semiconductor Structures* (New York: Academic)
[2] Leonard D, Krishnamurthy M, Reaves C M and Petroff P 1993 *Appl. Phys. Lett.* **63** 3203
[3] Oshinowo J, Nishioka M, Ishida S and Arakawa Y 1994 *Appl. Phys. Lett.* **65** 1421
[4] Koshiba S, Noge H, Akiyama H, Inoshita T, Nakamura Y, Shimizu A, Nagamune Y, Tsuchiya M, Kano H, Sakaki H and Wada K 1994 *Appl. Phys. Lett.* **64** 363
[5] Gustaffson A, Reinhardt F, Basiol G and Kapon E 1995 *Appl. Phys. Lett.* **67** 3673
[6] Hartmann A, Loubies L, Reinhardt F and Kapon E 1997 *Appl. Phys. Lett.* **71** 1314
[7] Watanabe S, Pelucchi E, Leifer K, Malko A, Dwir B and Kapon E 2005 *Appl. Phys. Lett.* **86** 243105
[8] Reinhardt F, Dwir B, Biasiol G and Kapon E 1997 *J. Cryst. Growth* **170** 689
[9] Volta A D, Vvedensky D D, Gogneau N, Pelucchi E, Rudra A, Dwir B, Kapon E and Ratsch C 2006 *Appl. Phys. Lett.* **88** 203104
[10] Ratsch C, Garcia J and Caflisch R E 2005 *Appl. Phys. Lett.* **87** 141901
[11] Ratsch C, Wheeler M C and Gyure M F 2000 *Phys. Rev.* B **62** 12636
[12] Murty M V R and Cooper B H 1999 *Phys. Rev. Lett.* **83** 352
[13] Ranguelov B, Altman M S and Markov I 2007 *Phys. Rev.* B **75** 245419
[14] Chung W F and Altman M S 2002 *Phys. Rev.* B **66** 075338
[15] Tan X, Ouyang G and Yang G W 2006 *Appl. Phys. Lett.* **88** 263116
[16] Tan X, Ouyang G and Yang G W 2006 *Phys. Rev.* B **73** 195322
[17] Weeks J D and Gilmer G H 1979 *Adv. Chem. Phys.* **40** 157
[18] Jones S H and Salinas L S 1995 *J. Cryst. Growth* **154** 163
[19] Kalff M, Comsa G and Michely T 1998 *Phys. Rev. Lett.* **81** 1255
[20] Pashley M D, Haberern K W and Gaines J M 1991 *Appl. Phys. Lett.* **58** 406
[21] Burton W K, Cabrera N and Frank F C 1951 *Phil. Trans. R. Soc.* A **243** 299